Methods in Ecology and Evolution

British Ecological Society

*Methods in Ecology and Evolution* 2015, **6,** 668–677 doi: 10.1111/2041-210X.12358

# A new method for resolving uncertainty of energy requirements in large water breathers: the 'mega-flume' seagoing swim-tunnel respirometer

**Nicholas L. Payne[1,2]*, Edward P. Snelling[3], Richard Fitzpatrick[4], Jamie Seymour[5], Robert Courtney[4], Adam Barnett[4,6], Yuuki Y. Watanabe[1,7], David W. Sims[8,9,10], Lyle Squire Jr[11] and Jayson M. Semmens[12]**

[1]*National Institute of Polar Research, Tachikawa, Tokyo 190-8518, Japan;* [2]*School of Biological, Earth and Environmental Sciences, University of New South Wales, Sydney, NSW 2052, Australia;* [3]*School of Biological Sciences, University of Adelaide, Adelaide, SA 5005, Australia;* [4]*School of Marine and Tropical Biology, James Cook University, Cairns, Qld 4878, Australia;* [5]*Australian Institute for Tropical Health and Medicine, James Cook University, Cairns, Qld 4878, Australia;* [6]*School of Life and Environmental Sciences, Deakin University, Burwood, Vic. 3125, Australia;* [7]*SOKENDAI (The Graduate University for Advanced Studies), Tachikawa, Tokyo 190-8518, Japan;* [8]*Marine Biological Association of the United Kingdom, Plymouth PL1 2PB, UK;* [9]*Ocean and Earth Science, National Oceanography Centre Southampton, University of Southampton, Southampton SO14 3ZH, UK;* [10]*Centre for Biological Sciences, University of Southampton, Southampton SO17 1BJ, UK;* [11]*Cairns Marine, Stratford, Qld 4870, Australia; and* [12]*Institute for Marine and Antarctic Studies, University of Tasmania, Hobart, Tas. 7001, Australia*

## Summary

**1.** Body size is a key determinant of metabolic rate, but logistical constraints have led to a paucity of energetics measurements from large water-breathing animals. As a result, estimating energy requirements of large fish generally relies on extrapolation of metabolic rate from individuals of lower body mass using allometric relationships that are notoriously variable. Swim-tunnel respirometry is the 'gold standard' for measuring active metabolic rates in water-breathing animals, yet previous data are entirely derived from body masses $< 10$ kg – at least one order of magnitude lower than the body masses of many top-order marine predators.

**2.** Here, we describe the design and testing of a new method for measuring metabolic rates of large water-breathing animals: a *c.* 26 000 L seagoing 'mega-flume' swim-tunnel respirometer. We measured the swimming metabolic rate of a 2·1-m, 36-kg zebra shark *Stegostoma fasciatum* within this new mega-flume and compared the results to data we collected from other *S. fasciatum* (3·8–47·7 kg body mass) swimming in static respirometers and previously published measurements of active metabolic rate measurements from other shark species.

**3.** The mega-flume performed well during initial tests, with intra- and interspecific comparisons suggesting accurate metabolic rate measurements can be obtained with this new tool. Inclusion of our data showed that the scaling exponent of active metabolic rate with mass for sharks ranging from 0·13 to 47·7 kg was 0·79; a similar value to previous estimates for resting metabolic rates in smaller fishes.

**4.** We describe the operation and usefulness of this new method in the context of our current uncertainties surrounding energy requirements of large water-breathing animals. We also highlight the sensitivity of mass-extrapolated energetic estimates in large aquatic animals and discuss the consequences for predicting ecosystem impacts such as trophic cascades.

**Key-words:** allometry, biomass, daily energy expenditure, ectotherm, feeding requirements, field metabolic rate, power curve, tuna, white shark, wind tunnel

## Introduction

Metabolic rate is fundamental to all biological processes (Brown *et al.* 2004) as it describes the transformation of energy within organisms and its flow throughout ecosystems. It is the currency that sets the magnitude of energy flux between trophic levels and is therefore a central parameter underpinning predator–prey interactions, and the cascading effects of changing population abundances in high (i.e. top-down; Heithaus *et al.* 2008; Baum & Worm 2009) and low (bottom-up; Ware & Thomson 2005) trophic positions.

Marine predators occupying high trophic positions are declining at a rapid pace world-wide (Hutchings & Baum 2005;

*Correspondence author. E-mail: n.payne@unsw.edu.au

Heithaus *et al*. 2008), and these declines have been implicated as driving severe cascading effects throughout lower trophic levels (Estes *et al*. 1998; Frank *et al*. 2005; Myers *et al*. 2007). As a consequence, much contemporary research aims to quantify impacts of declining top-order predators, and to predict likely responses at the community level and ecosystem level. Ecosystem models are the most common method for interpreting and predicting consequences of declining upper trophic levels (Heithaus *et al*. 2008), and these are underpinned by system-specific parameterisation. For the group of animals implicated as driving the most severe trophic cascades (large marine predatory fishes), one of the principal knowledge gaps is direct measurements of their energy requirements (Borer *et al*. 2005; Hunsicker *et al*. 2011). Clearly, this represents a major limitation for accurately predicting the consequences of the declines documented throughout the oceans (Pauly *et al*. 1998; Myers *et al*. 2007).

Because direct measurements are scarce, a common approach to estimating energy requirements in large marine animals is to quantify the relationship between metabolism and body mass in smaller animals, and extrapolate upwards. This approach has been used to infer impacts on lower trophic levels in both fishes and mammals (Estes *et al*. 1998; Williams *et al*. 2004; Semmens *et al*. 2013). However, attempts to identify a universal relationship between body mass and metabolic rate (generally represented by a power curve, $aM^b$, where $M$ is body mass, $a$ is the elevation, and $b$ is the scaling exponent) have been highly controversial for the better part of a century (*c*. Kleiber 1932), with recent findings suggesting the scaling exponent varies greatly between taxa (DeLong *et al*. 2010; White, Frappell & Chown 2012; Hudson, Isaac & Reuman 2013), with lifestyle and temperature (Killen, Atkinson & Glazier 2010) and activity level (Glazier 2005, 2010), and that allometric power curves may not describe the relationship between body size and metabolism at all (Savage, Deeds & Fontana 2008; Kolokotrones *et al*. 2010). These considerations suggest the lack of metabolic rate measurements from large animals is not only a hindrance to describing the laws governing biological allometry, but also that extrapolated estimates of metabolism in large animals are prone to inaccuracy. For mass-balance ecosystem models of declining upper trophic levels, the consequences of such inaccuracies could be severe.

Swim-tunnel respirometry (Brett 1967) is the 'gold standard' for measuring active metabolic rates in water-breathing animals, as it enables energetic measurements across a range of swimming speeds. This attribute informs comparisons as fundamental as the differential costs of locomotion across animal groups (Schmidt-Nielsen 1972) and also facilitates estimation of field metabolic rate when swimming speed is calibrated against heart rate or acceleration (Wilson *et al*. 2006; Halsey *et al*. 2008; Payne *et al*. 2011), and these parameters are then collected from wild animals. Logistical and engineering constraints have limited the size of swim-tunnel respirometers, such that we are not aware of any studies having used animals larger than 10 kg body mass (the largest specimens of which we are aware were tunas and mako sharks of almost 10 kg mass; Blank *et al*. 2007; Sepulveda, Graham & Bernal 2007). Given many top-order marine animals are at least one order of magnitude larger than this, swim-tunnel respirometers that allow for measurements in larger (upwards of 100 kg) water-breathing animals would represent an extremely powerful tool for the fields of trophic ecology and fisheries sciences. Large-animal data would also significantly inform the ongoing body mass–metabolism debate, which is a topic with deep ecological significance (Brown *et al*. 2004). Perhaps, symptomatic of the logistical barriers associated with estimating energetics in large animals, a literature search suggests scientific interest in trophic cascades and metabolic scaling are both steadily increasing, whereas no detectable concomitant increase in the frequency of field metabolic rate studies has occurred over the past 20 years (Fig. 1). Since activity level has a major impact on an animal's energy budget, such a trend highlights the pressing need for technological and conceptual advances in how we measure, and estimate, active metabolism of large aquatic animals for providing new empirical data to inform energetic and trophic models.

Here, we report the construction and successful trial of a *c*. 26 000 L sea-going Brett-type swim-tunnel respirometer capable of accommodating animals >100 kg body mass, and measuring oxygen consumption (as a proxy of metabolic rate) within their natural habitat. We compare metabolic rate measurements from a zebra shark *Stegostoma fasciatum* (2·1 m length, 36 kg body mass) swum in the 'mega-flume' to measurements we collected from the same species (3·8–47·7 kg body mass range) during routine swimming trials in static respirometers. We also compare our data for *S. fasciatum* to previous metabolic rate measurements in sharks from other species. In emphasising the power of this new physiological tool, we highlight the dangers associated with extrapolating energetic estimates from low body masses and present a case for the need to measure metabolic rates directly in large water-breathing animals.

## Materials and methods

### MEGA-FLUME CONSTRUCTION

The mega-flume was constructed in the style of a submersible Brett-type respirometer that can be separated into six segments (Fig. 2; see Appendix S1 for notes on design and logistics). Four segments were 2·44 m long with a square cross section of 1·22 × 1·22 m, and the two end segments had the same cross-sectional area but were curved with external radius of 1·83 m (internal radius 0·61 m), to give a total flume volume of 25 935 L. The flume frame was constructed of 25-mm (square cross section) aluminium (3 mm thick) connected by plastic snap-lock fittings, and the main body of the flume was constructed of 1·5 mm (for straight sections) and 3·0-mm (for the curved ends) polycarbonate sheet. The polycarbonate sheet was connected to the aluminium frame via 3-mm rubber gaskets secured by blind rivets to create a watertight seal. To enhance the structural integrity of the curved ends, 3-mm aluminium plates were welded onto the frame on the top and bottom of each end segment. These plates were 1·83 × 3·66 m wide and were internally welded to curved aluminium fixtures which were riveted to the curved polycarbonate sheets. Each curved segment had a

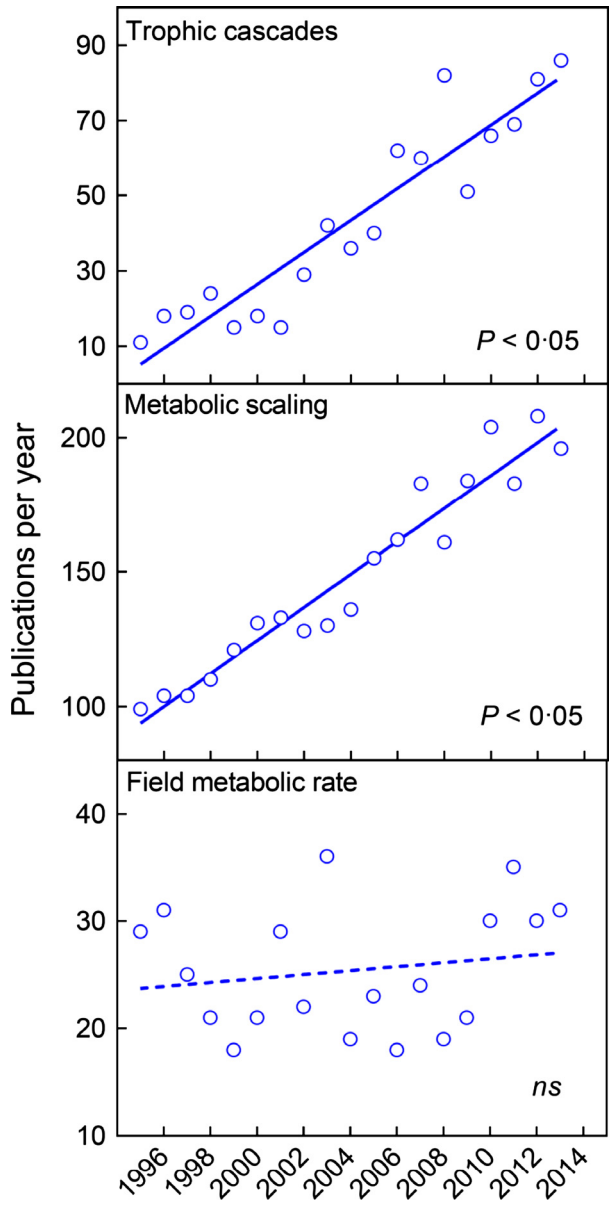


**Fig. 1.** Research trends. Number of published studies examining trophic cascades, metabolic scaling and field metabolic rate identified through an ISI Web of Science search using the following terms: top panel = ['trophic cascade']; second panel = ['metabolic rate' AND 'body mass']; third panel = ['field metabolic rate'] OR ['field energetics'] OR ['daily energy expenditure' AND 'animal* OR ecology']. The search was restricted to the past 20 years, and trends were examined with linear regression. Data were not standardised by overall trends in journal publication rates, so the lack of increase for field metabolic rate suggests a relative decrease in focus for this field. Slopes indicate an increase of 4·2 and 6·1 publications per year for trophic cascades and metabolic scaling, respectively.

further two curved polycarbonate sheets, in parallel to the first, which reduced turbulence within the swim chamber section. To further reinforce the mega-flume, two additional aluminium bars were constructed around the outside of each straight segment. Segments of the mega-flume are connected to one another via stainless nuts and bolts (which were easily hand-tightened) through the aluminium frame, and the interface of each segment being sealed by 10-mm waterproof adhesive foam gasket. While the four straight segments are somewhat flexible and easy to manipulate into place when independent of one another, securing all six segments together provides a highly robust structure that may withstand many types of oceanic conditions.

We built two hatches into the lateral side of the swim chamber section – one fore and one aft – to facilitate introduction and removal of animals. These square hatches were constructed of the same materials as the swim chamber and were connected to the chamber via 10-mm gasket and quick-release latches. These latches enable rapid removal of the animal if necessary.

Water flow was controlled via four electric water pumps (3 × 2·2 and 1 × 1·9 kW; BX series; Austral Pool Ltd., Noble Park, Victoria, Australia), with each pump drawing water through 0·5-m long manifolds attached to the section of the flume opposite the swim chamber (Fig. 2) via 40-mm skin fittings. Each of the four manifolds was attached to one side of the flume, and drew water from a series of holes facing upstream. The intake hose was 50 mm in diameter and non-compressible, whereas the return hose was 50-mm 'flatpack'. Water was returned to the flume via 4 × 40 mm skin fittings with 90° threaded nozzles facing downstream and approximately 1·2 m downstream of the intake manifolds. Such a configuration created four powerful jets of water running parallel to the length of the flume that achieved relatively homogenous water velocities throughout the cross-sectional area of the swimming section up to approximately 0·50 m $s^{-1}$. Water velocity was initially quantified throughout the cross-sectional area of the swimming chamber using an open channel velocity metre (model 001; Valeport Ltd, Devon, UK) and then continuously by fixing the velocity metre in the centre of the cross-sectional area at the downstream end of the swim chamber (Fig. 2). We did not account for solid blocking effects because the shark represented <10% of the flume cross-sectional area (Bell & Terhune 1970).

The light-weight construction materials enabled each segment to be carried by 2–4 researchers with relative ease, and 4–6 buoys of intermediate size are sufficient to maintain flotation of the mega-flume at the surface.

## MEGA-FLUME TRIAL WITH 2·1-M ZEBRA SHARK *S. FASCIATUM*

The mega-flume was assembled in a vacant berth (*c.* 5 m water depth) at Yorkeys Knob Marina (35·70°S, 150·179°E). This small marina experiences significant (*c.* 1–2 m) tidal exchange with the Coral Sea and therefore maintains relatively high water quality. A 2·1 m (total length, TL), 36·0-kg *S. fasciatum* was transported from commercial holding tanks at Cairns Marine (www.cairnsmarine.com) via a 1000-L transport container which was continuously aerated with pure oxygen during the 10-min journey. This shark was collected from a reef near Cairns and subsequently maintained in captivity to commercial standards. *S. fasciatum* can actively ventilate their gills via buccal pumping (Dudgeon, Lanyon & Semmens 2013) and are one of the more docile shark species to handle (LSJ, pers. obser.). This individual in particular was considered a good subject for initial testing of the mega-flume because while approximately fourfold larger than fish previously swum in such a device, it was within the lower range of body sizes that could be swum in the mega-flume, and was therefore a better test of the precision of the respirometry system than a large specimen with a higher metabolic rate.

The shark was carried in a cradle from the transport container to the mega-flume and immediately placed within the working section via the lateral rear entry hatch (Fig. 2). The hatch was sealed, and the seawater pumps were successively engaged. The shark appeared to swim com-

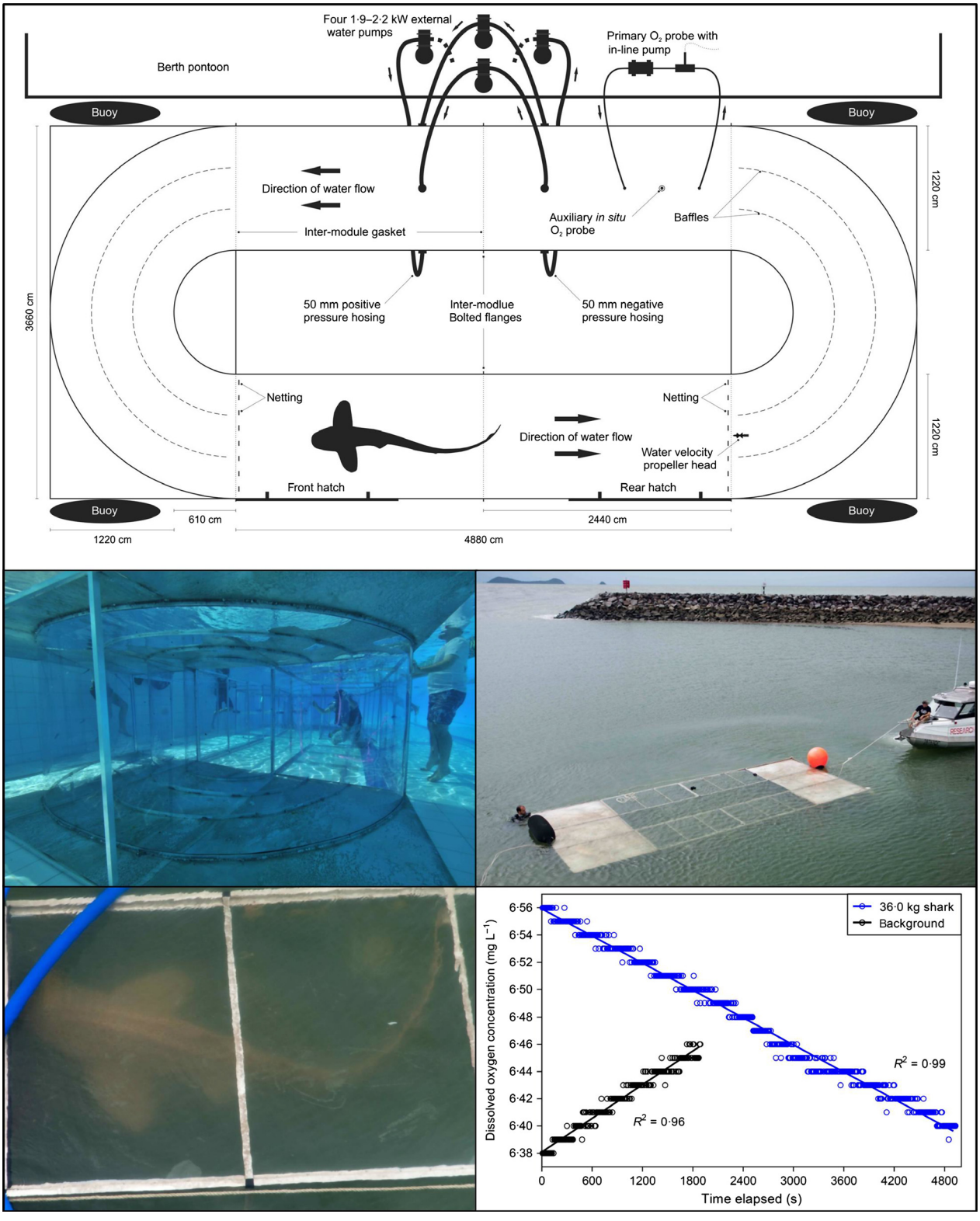


**Fig. 2.** Main panel: schematic of *c*. 26 000 L mega-flume submersible swim-tunnel respirometer. Middle panels: initial tests and transport to Yorkeys Knob marina. Bottom panels: respirometry trial and raw oxygen traces (blue for the shark trial and black for the post-trial period) for a 2·1-m, 36·0-kg zebra shark *Stegastoma fasciatum*. See Movie S1 of swim trial.

fortably (maintaining position near the front of the swim chamber) with three of the four pumps operating, at a nominal speed of 0·4 m $s^{-1}$ (see Movie S1), so this speed was maintained throughout the trial, which lasted 80 min. After the trial, the shark was removed from the mega-flume and weighed, and the mega-flume was immediately resealed. Oxygen concentration was measured for a further

40 min (with the flume running at the same speed as for the animal trial) to control for background respiration and exchange between the mega-flume and the external environment, and this background variation was subtracted from the rate calculated for the swim trial.

Oxygen concentration and water temperature were monitored with two separate probes (both LDO101 model with HQ40d multiparameter meter; Hach™, Loveland, CO, USA). The first probe was mounted directly on the mega-flume, with the sensor positioned approximately 0·1 m below the upper surface. The second probe was fixed within a small (*c*. 100 mL) sealed sump on the berth pontoon, with water drawn from the centre of the mega-flume cross-sectional area by a small aquarium pump and hose, and returned by another hose. Both samples were taken from the section of the mega-flume opposite the working section (Fig. 2), and measurements from each probe were compared to one another to evaluate potential stratification in oxygen concentration within the mega-flume. Both probes had a sampling frequency of 0·1 Hz, a manufacturer-reported accuracy of 0·1 mg $L^{-1}$, and were calibrated to 100% oxygen saturation in air prior to the swim trial.

Our primary objective was to evaluate the operation of the mega-flume, so we chose to swim the shark continually upon entry into the working section. Given a lack of acclimation period and measurement of resting metabolic rate, we consider our metabolic data to be most accurately described as 'active swimming metabolic rate', rather than 'routine'. As such, we considered the most appropriate way to evaluate the accuracy of our mega-flume data was to compare it to data collected under similar experimental procedures.

### INTRA- AND INTERSPECIFIC COMPARISONS

The active metabolic rates of six *S. fasciatum* (body masses of 3·8, 4·4, 16·0, 18·7, 22·0 and 47·7 kg) were measured within static respirometry chambers at Cairns Marine. These sharks were carried from their holding tanks to a 3800-L circular tank that was subsequently sealed with plastic sheeting. As with the mega-flume trial, oxygen concentration was measured as soon as the shark was placed in the respirometer, and for all trials, sharks swam continually around the perimeter of the tank at their chosen speed. A water pump was fixed to the bottom of the respirometer to maintain gentle centrifugal flow, and given all sharks swam continuously, we considered oxygen to be well mixed during each trial. All trials lasted approximately 45 min, and readings from the last 5–10 min were used to calculate oxygen consumption rates for each shark. A 25-min control run was carried out after the last respirometry measurement, and any background respiration rate was subtracted from the animal measurements. The same probe model was used for these trials as for the mega-flume trial, and for both experiments (static respirometer and mega-flume), the water temperature remained at 27·5 ± 1°C and oxygen above 80% saturation (assuming 6·56 mg $L^{-1}$ in saturated seawater).

To compare our results with literature values, we compiled measurements of shark metabolic rate from studies that allowed animals to swim at their preferred speeds. We only included those studies that report continuous, animal-selected swimming speeds and standardised all data to a temperature of 20°C using a $Q_{10}$ of 1·65 as previously reported for fish standard metabolic rate (White, Phillips & Seymour 2006). Metabolic rate (mg $O_2$ $h^{-1}$) and body mass (kg) data were $\log_{10}$-transformed and analysed with linear mixed models (IBM SPSS version 22), using restricted maximum likelihood estimation and treating species as the random effect (after Hudson, Isaac & Reuman 2013). Using this method, the exponent (*b*) becomes the slope in a linear regression of $\log_{10}$-transformed body mass (*M*) and metabolic rate, and *a* becomes the antilog of the intercept. $\text{Log}_{10}$-transformation is considered appropriate where errors are multiplicative, as is often the case for metabolic scaling data (Xiao *et al*. 2011).

To highlight the sensitivity of metabolic rate estimates calculated by extrapolation from relatively low body masses, we fitted several other models to our data. For these, we maintained the intercept that was estimated from our mixed-effects model, but adjusted the slope in line with several theoretical values: 0·67 after the surface law of metabolism (Rubner 1883); 0·75 after Kleiber's law (Kleiber 1932); and 0·89 after a comparative analysis of field metabolic rate in ectotherms (i.e. reptiles; Nagy 2005).

## Results

### MEGA-FLUME TRIAL

We experienced little difficulty moving the *S. fasciatum* into and out of the mega-flume, and observed no obvious signs of stress, with steady swimming apparent over the entire 80-min trial. The nominal speed for the *S. fasciatum* mega-flume experiment was 0·40 m $s^{-1}$; a speed that remained relatively constant throughout the trial (fluctuating between 0·37 and 0·43 m $s^{-1}$). Oxygen concentration declined linearly from *c*. 6·55 to 6·40 mg $L^{-1}$, with little to suggest a variable rate of oxygen consumption ($R^2$ = 0·99 for a linear fit to data for the entire 80-min trial; Fig. 2). There was a linear increase in oxygen concentration after removal of the animal (Fig. 2), suggesting a degree of oxygen flux into the mega-flume from the environment. This was likely due to the presence of a small (*c*. 0·5 × 20 cm) gap between two flume segments caused by damage to that section of gasket, which occurred as the flume was being assembled. Prior to the swim trial, we ensured that this area of the flume was firmly secured and that the remaining gasket could not change position. This ensured that the leak was consistent throughout the entire experimental period, and we corrected for the increase in oxygen concentration during our background trial using standard methods (Fig. 2). After this correction, the calculated metabolic rate of the 36·0-kg *S. fasciatum* at 27·5°C was 6995 mg $O_2$ $L^{-1}$ $h^{-1}$ (Fig. 3 inset; red circle).

### INTRA- AND INTERSPECIFIC COMPARISONS

Sharks within the static respirometry chamber swam continuously around its perimeter during all trials, and oxygen declined steadily for each individual (Fig. S1). After correcting for a small decrease in oxygen concentration upon removal of the animals from the chamber (likely a result of microbial respiration), $\log_{10}$-transformed metabolic rate measurements for the six *S. fasciatum* within the static respirometry chamber scaled linearly with $\log_{10}$-transformed mass, and the mega-flume data were highly consistent with these determinations (the mega-flume datum fell well within 95% confidence intervals generated from the six static respirometer data; $P < 0{\cdot}05$, $R^2$ = 0·98 and exponent = 0·80 for the seven data combined; Fig. 3 inset).

Our literature search returned four studies of preferred-swimming metabolic rates in sharks, and these temperature-

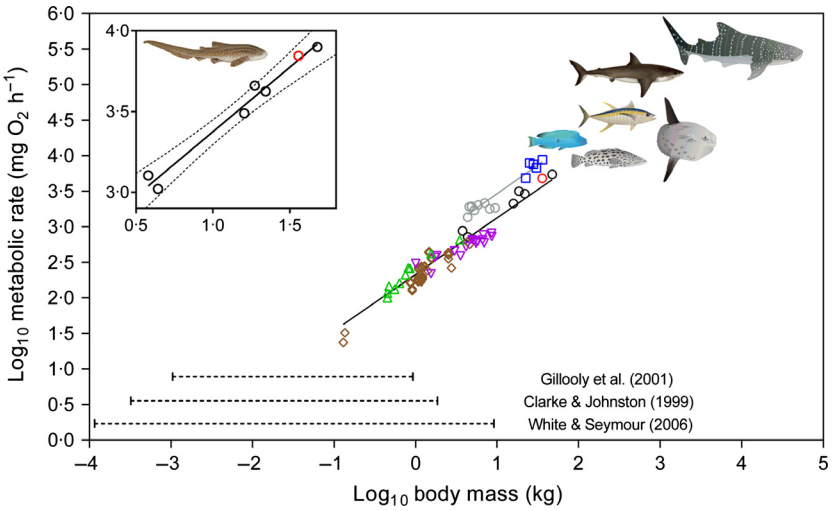


**Fig. 3.** Preferred-swimming metabolic rate data in the main panel (brown symbols for bonnethead sharks *Sphyrna tiburo*; Parsons 1990; green for blacknose sharks *Carcharhinus acronotus*; Carlson, Palmer & Parsons 1999; purple for sandbar sharks *Carcharhinus plumbeus*; Dowd *et al*. 2006; grey for mako sharks *Isurus oxyrinchus*; Sepulveda, Graham & Bernal 2007; blue for white sharks *Carcharodon carcharias*; Ezcurra *et al*. 2012; black for *Stegostoma fasciatum* swum in static respirometers and red for the mega-flume [this study]) were standardised to 20°C using a $Q_{10}$ of 1·65 (White, Phillips & Seymour 2006), whereas data inset (for *S. fasciatum*) is presented at the temperature of measurement (27·5°C). Regionally endothermic white and mako sharks were excluded from the main (black) regression line due to their regional endothermy. Mixed-effects modelling of remaining data estimated a slope of 0·79. The upper truncation of fish body masses from which metabolic rate data have been previously collected are emphasised by plotting (i) the fish mass range used in several influential comparative studies of mass–metabolism allometry (dashed lines) and (ii) the approximate mass of several large bodied fishes. Grey symbols for *I. oxyrinchus* represent the largest fish previously measured in a swim-tunnel respirometer of which we are aware. In this figure, all except the red (*S. fasciatum* in the mega-flume) and grey (for *I. oxyrinchus* swum in a swim tunnel) data are for sharks swimming at their preferred speeds.

standardised data are presented in Fig. 3 (main panel). The mass ranged from a 0·13-kg bonnethead shark *Sphyrna tiburo* (Parsons 1990) to a 36·2-kg white shark *Carcharodon carcharias* (Ezcurra *et al*. 2012). Given the regionally endothermic physiology of white sharks, we expected their metabolic rates to be significantly higher than the remaining ectothermic animals (including our *S. fasciatum*) and temperature standardisation for heterothermic fish may be prone to error, so we excluded those data from our models. Remaining data included the *S. tiburo*, blacknose sharks *Carcharhinus acronotus* (Carlson, Palmer & Parsons 1999) and sandbar sharks *Carcharhinus plumbeus* (Dowd *et al*. 2006), with the full data set consisting of 65 measurements over a body mass range spanning nearly two orders of magnitude (Fig. 3, main panel).

The mixed-effects model of $\log_{10}$-metabolic rate revealed a significant linear increase with $\log_{10}$-mass ($P < 0{\cdot}05$), with a slope of 0·78 and an intercept of 2·31 for the previously published shark data. Our temperature-standardised *S. fasciatum* data were consistent with linear extrapolation from the lower body masses of the earlier data, with inclusion of these seven data elevating the slope only slightly to 0·79 (Fig. 3, main panel). For visual comparison, we plotted the white shark data (blue squares) alongside our data set, and data from the similarly regionally endothermic mako shark *Isurus oxyrinchus* (grey circles; Sepulveda, Graham & Bernal 2007). While the mako shark data were derived from animals swimming at a controlled speed in a swim-tunnel respirometer (and therefore not directly comparable to all other data), to our knowledge these animals represent the largest fish (1·07 m TL; 9·5 kg body mass) ever swum in such a device previously. Inclusion of these data serves to illustrate the upper truncation of body masses from which respirometry data have previously been collected for fishes.

Our conceptual illustration of the influence of variable allometric slopes on extrapolated estimates of whole-animal metabolic rates is presented in Fig. 4. Whole-animal estimates vary markedly depending on the exponent used, with the relative difference increasing with body mass. For example, whole-animal metabolism of a 20-kg fish (e.g. blue shark *Prionace glauca*, Fig. 4 top right panel) estimated using an exponent of 0·89 (after Nagy 2005) is 1·93 times higher than if 0·67 is used (after the surface law of metabolism; Rubner 1883). This error increases with body mass, such that estimates for a 5000-kg whale shark *Rhincodon typus* can be almost 6·5 times higher depending on the exponent used (factorial difference of 6·46 for exponents of 0·67 and 0·89; Fig. 4 bottom panel). Even intermediate differences in exponents can lead to large differences in extrapolated estimates; 0·75 will provide estimates of metabolism 1·3 and 2·0 times higher than those calculated using an exponent of 0·67 for a 20- and 5000-kg animal, respectively.

## Discussion

Our large, submersible swim-tunnel respirometer enabled measurements of metabolic rate to be made in the largest water-breathing animal – by a significant margin – to have been placed in such a device (Fig. 3, main panel), with intra- and interspecific comparisons indicating a high degree of accuracy was achieved using this new tool. Despite the novelty of the

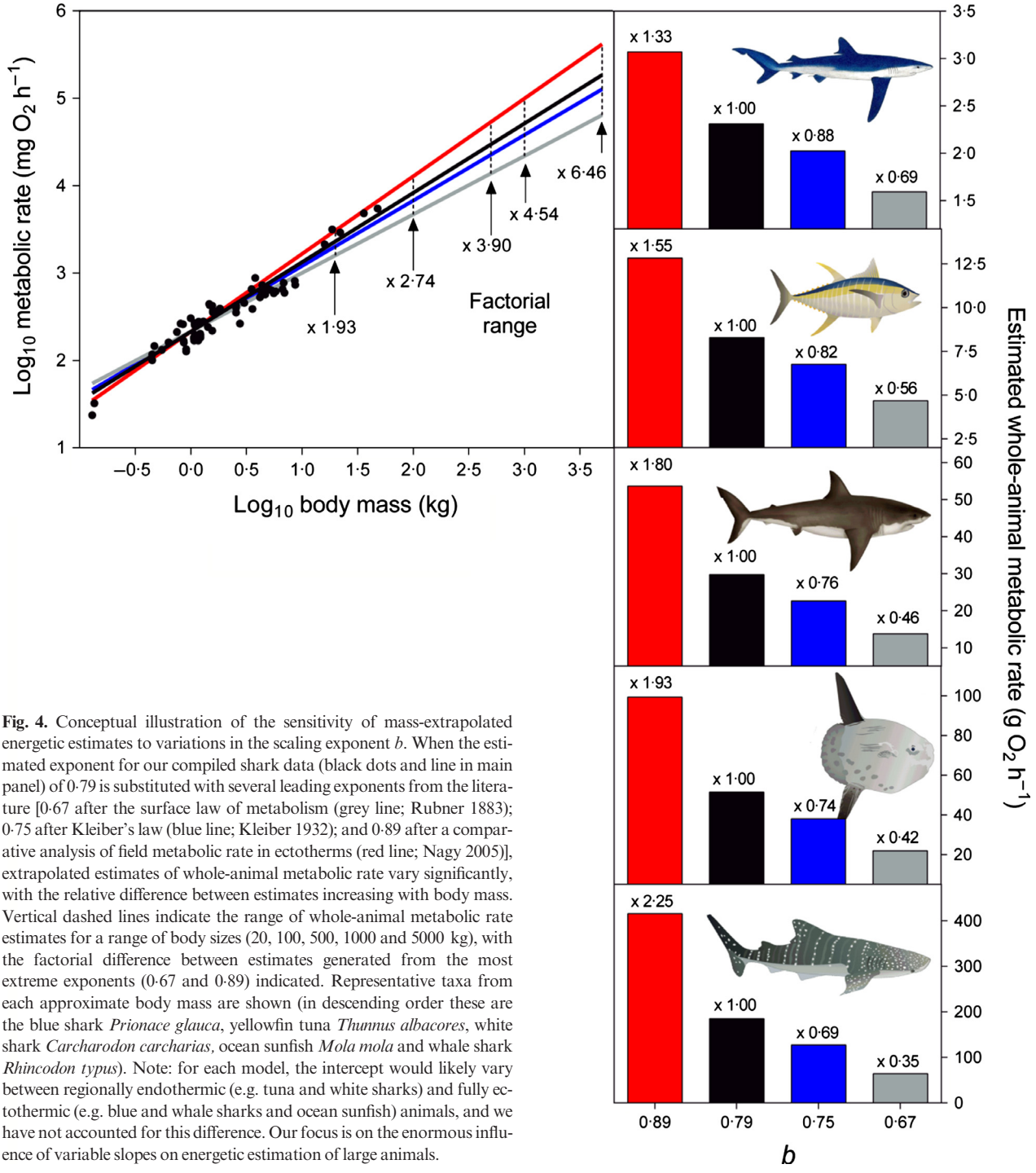


**Fig. 4.** Conceptual illustration of the sensitivity of mass-extrapolated energetic estimates to variations in the scaling exponent *b*. When the estimated exponent for our compiled shark data (black dots and line in main panel) of 0·79 is substituted with several leading exponents from the literature [0·67 after the surface law of metabolism (grey line; Rubner 1883); 0·75 after Kleiber's law (blue line; Kleiber 1932); and 0·89 after a comparative analysis of field metabolic rate in ectotherms (red line; Nagy 2005)], extrapolated estimates of whole-animal metabolic rate vary significantly, with the relative difference between estimates increasing with body mass. Vertical dashed lines indicate the range of whole-animal metabolic rate estimates for a range of body sizes (20, 100, 500, 1000 and 5000 kg), with the factorial difference between estimates generated from the most extreme exponents (0·67 and 0·89) indicated. Representative taxa from each approximate body mass are shown (in descending order these are the blue shark *Prionace glauca*, yellowfin tuna *Thunnus albacores*, white shark *Carcharodon carcharias,* ocean sunfish *Mola mola* and whale shark *Rhincodon typus*). Note: for each model, the intercept would likely vary between regionally endothermic (e.g. tuna and white sharks) and fully ectothermic (e.g. blue and whale sharks and ocean sunfish) animals, and we have not accounted for this difference. Our focus is on the enormous influence of variable slopes on energetic estimation of large animals.

data with respect to body size, a 36-kg shark represents an animal on the lower end of the body mass range that could feasibly be measured within the device. As such, mega-flumes have the potential to largely resolve the upper truncation of aquatic animal body masses from which we have a reasonable understanding of energetics (Fig. 3, main panel). This would represent a significant advance towards understanding the mechanisms driving variability in the mass–metabolism relationship between animal groups (DeLong *et al.* 2010; White, Frappell & Chown 2012; Hudson, Isaac & Reuman 2013), and in doing so, remove much of the uncertainty surrounding energy requirements of large, water-breathing animals. Addressing this uncertainty is critical with respect to the accuracy of predictive ecosystem models, and our current degree of uncertainty appears to be large.

Allometric curves are nonlinear, such that the relative magnitude of the differences between body mass–metabolism curves increases as body mass increases. As illustrated in Fig. 4, fitting of several commonly cited exponents to the $\log_{10}$-mass vs. $\log_{10}$-metabolism relationship for our compiled

shark data suggests each exponent (except perhaps 0·67) could represent the data equally well under relatively minor changes to the data set. However, when each model is extrapolated to estimate whole-animal metabolic rates of larger body masses (Fig. 4 vertical dashed lines, with estimates in panels on right), it is clear that even intermediate variations in the exponent (e.g. 0·79 vs. 0·89) lead to dramatic differences in subsequent estimates, with the relative magnitude of these differences increasing with mass (Fig. 4 main panel). From a published example (Semmens *et al.* 2013), estimates of field metabolic rate in 428-kg white sharks *Carcharodon carcharias* were extrapolated upwards from smaller (<40 kg) mako and white sharks using the mean exponent identified in a comparative analysis of fish resting metabolic rate (0·79; Clarke & Johnston 1999). The estimate of daily energy expenditure (28·2 MJ day$^{-1}$) from Semmens *et al.* (2013) is 55% lower than would be estimated if metabolic rate were extrapolated upwards using the mean exponent identified in a comparative analysis of ectotherm field metabolic rate (0·89; Nagy 2005). As a result, the advantages of white sharks targeting seasonally abundant seal pups that was identified by Semmens *et al.* (2013) is less obvious if a higher exponent is used (it becomes more likely that predation on more than one seal pup per day is required to contribute significant energy to growth). In another study, field metabolic rates in killer whales *Orcinus orca* were extrapolated upwards from that of pinnipeds and dolphins with an exponent of 0·756, and these estimates were then used to predict the likely impacts of *O. orca* on lower trophic levels (Williams *et al.* 2004). Replacement of their exponent with the mean from a recent comparative analysis of field metabolic rates from a variety of mammal taxa (0·64; Hudson, Isaac & Reuman 2013) generates metabolic rate values 60–63% lower than the published estimates. These examples are not intended to question the findings of those previous studies (e.g. phylogeny is an important consideration, and Hudson *et al.* found the taxa relevant to the Williams study had a higher exponent than their average of 0·64), but rather to illustrate that the choice of different scaling exponents for extrapolating energetic estimates can have major implications for subsequent interpretations.

The simple points described above may be well recognised in some fields (e.g. comparative physiology), but with the significant variation in the scaling exponent for resting and active metabolism seen across animal groups (DeLong *et al.* 2010; White, Frappell & Chown 2012; Hudson, Isaac & Reuman 2013), the sensitivities associated with extrapolating from low body masses (Fig. 4), and the paucity of direct measurements from large fully aquatic animals (Fig. 3), it would be difficult to argue that our understanding of energetics in large marine predators is anything other than uncertain. One approach to resolving this uncertainty is to continue exploring the most appropriate model fits to metabolic scaling across animal groups, and no doubt this pursuit will continue. For example, recent advances in the ability to include phylogenetic information in scaling models have improved confidence in the allometric scaling of metabolism across animal groups (Garland, Harvey & Ives 1992; Halsey, Butler & Blackburn 2006; White, Blackburn & Seymour 2009). Another very useful avenue of research will be to expand empirical metabolic rate determinations for aquatic animals with large body mass, and the method described here will help facilitate such an advance.

The logistical and financial scale of the mega-flume is not prohibitive but may restrict the broad adoption of our approach to some degree; however, multi-institutional collaborative efforts could bring this type of infrastructure to the forefront of future studies that measure metabolic rates in large water-breathing animals. The relative ease of transport and seaworthiness of the device (see Appendix S1) facilitates application to a broad range of species, and depending on oceanic conditions, there is little to inhibit long (*c.* 12–24 h) post-capture acclimation periods, such that effects of stress can be reduced, and robust measures of standard metabolic rate can be obtained. Alterations to flume design (e.g. narrowing of the internal cross section of the swim chamber and reconfiguration of the pump system) would allow higher attainable water velocities, which would be useful for manipulating a broader range of swimming speeds in active species such as lamnid sharks and tuna. While temperature would be difficult to manipulate in a natural setting (our flume is highly conductive), the possibilities of manipulating oxygen concentrations or pH are exciting, particularly for tests of acute physiological responses under current climate forecasts (Rosa & Seibel 2008; Seibel 2011; Stramma *et al.* 2012).

Together with several emerging approaches to quantifying ingestion rates (Meyer & Holland 2012; Naito *et al.* 2013; Watanabe & Takahashi 2013) and activity levels (Wilson *et al.* 2006; Payne *et al.* 2013, 2014) in free-ranging animals, our new tool has potential to fill a large void in our understanding of the energy requirements of large water-breathing animals. This research gap represents a barrier to understanding the physical laws governing allometric scaling of animal metabolism in general, and so in the energetic benefits of obtaining large size in the first place (Halsey, Butler & Blackburn 2006; Kolokotrones *et al.* 2010; Ruxton 2011). The animals of which we know little of their energy requirements are the same group that are disappearing from our oceans at a rapid pace, and are implicated as driving severe cascading effects throughout ecosystems. Clearly, the development of approaches such as ours is critical to improving our understanding of the role of these apex predators in our changing oceans.

## Acknowledgements

Thanks Barb and Wayne Williams, Sandy Taylor and the students at JCU for assistance with flume construction and logistics, and staff at Cairns Marine for helping with shark transport and handling. Thanks Alfie Payne for early discussion on flume design, and Martin Lambert at Adelaide University for provision of the current metre. Animal use was facilitated by a University of Tasmania ethics permit (number A12578).

## Author contributions

NLP and EPS conceived the mega-flume, and RF led its construction. All authors performed the experiments and/or interpreted the results, NLP analysed the data and drafted the manuscript and all authors contributed to its final form.

## Funding

Funding was provided by OceansIQ, and NLP was supported by a postdoctoral fellowship from the Japan Society for the Promotion of Science (P13749).

## Data accessibility

All data are included in the text or as Supporting information.

## References

Baum, J.K. & Worm, B. (2009) Cascading top-down effects of changing oceanic predator abundances. *Journal of Animal Ecology*, **78**, 699–714.

Bell, W.H. & Terhune, L.B. (1970) Water tunnel design for fisheries research. Fisheries Research Board of Canada Technical Report.

Blank, J.M., Farwell, C.J., Morrissette, J.M., Schallert, R.J. & Block, B.A. (2007) Influence of swimming speed on metabolic rates of juvenile Pacific bluefin tuna and yellowfin tuna. *Physiological and Biochemical Zoology*, **80**, 167–177.

Borer, E.T., Seabloom, E.W., Shurin, J.B., Anderson, K.E., Blanchette, C.A., Broitman, B., Cooper, S.D. & Halpern, B.S. (2005) What determines the strength of a trophic cascade? *Ecology*, **86**, 528–537.

Brett, J.R. (1967) Swimming performance of sockeye salmon (*Oncorhynchus nerka*) in relation to fatigue time and temperature. *Journal of the Fisheries Research Board of Canada*, **24**, 1731–1741.

Brown, J.H., Gillooly, J.F., Allen, A.P., Savage, V.M. & West, G.B. (2004) Toward a metabolic theory of ecology. *Ecology*, **85**, 1771–1789.

Carlson, J.K., Palmer, C.L. & Parsons, G.R. (1999) Oxygen consumption rate and swimming efficiency of the blacknose shark, *Carcharhinus acronotus*. *Copeia*, **1**, 34–39.

Clarke, A. & Johnston, N.M. (1999) Scaling of metabolic rate with body mass and temperature in teleost fish. *Journal of Animal Ecology*, **68**, 893–905.

DeLong, J.P., Okie, J.G., Moses, M.E., Sibly, R.M. & Brown, J.H. (2010) Shifts in metabolic scaling, production, and efficiency across major evolutionary transitions of life. *Proceedings of the National Academy of Sciences of the United States of America*, **107**, 12941–12945.

Dowd, W.W., Brill, R.W., Bushnell, P.G. & Musick, J.A. (2006) Standard and routine metabolic rates of juvenile sandbar sharks (*Carcharhinus plumbeus*), including the effects of body mass and acute temperature change. *Fishery Bulletin*, **104**, 323–331.

Dudgeon, C.L., Lanyon, J.M. & Semmens, J.M. (2013) Seasonality and site fidelity of the zebra shark, *Stegostoma fasciatum*, in southeast Queensland, Australia. *Animal Behaviour*, **85**, 471–481.

Estes, J.A., Tinker, M.T., Williams, T.M. & Doak, D.F. (1998) Killer whale predation on sea otters linking oceanic and nearshore ecosystems. *Science*, **282**, 473–476.

Ezcurra, J.M., Lowe, C.G., Mollet, H.F., Ferry, L.A. & O'Sullivan, J.B. (2012) Oxygen consumption rate of young-of-the-year white sharks, *Carcharodon carcharias*, during transport to the Monterey Bay Aquarium. *Global Perspectives on the Biology and Life History of the White Shark* (ed. M.L. Domeier), pp. 17–26. CRC Press, Boca Raton.

Frank, K.T., Petrie, B., Choi, J.S. & Leggett, W.C. (2005) Trophic cascades in a formerly cod-dominated ecosystem. *Science*, **308**, 1621–1623.

Garland, T., Harvey, P.H. & Ives, A.R. (1992) Procedures for the analysis of comparative data using phylogenetically independent contrasts. *Systematic Biology*, **41**, 18–32.

Glazier, D.S. (2005) Beyond the '3/4-power law': variation in the intra- and interspecific scaling of metabolic rate in animals. *Biological Reviews*, **80**, 611–662.

Glazier, D.S. (2010) A unifying explanation for diverse metabolic scaling in animals and plants. *Biological Reviews*, **85**, 111–138.

Halsey, L.G., Butler, P.J. & Blackburn, T.M. (2006) A phylogenetic analysis of the allometry of diving. *The American Naturalist*, **167**, 276–287.

Halsey, L.G., Shepard, E.L.C., Hulston, C.J., Venables, M.C., White, C.R., Jeukendrup, A.E. & Wilson, R.P. (2008) Acceleration versus heart rate for estimating energy expenditure and speed during locomotion in animals: tests with an easy model species, *Homo sapiens*. *Zoology*, **111**, 231–241.

Heithaus, M.R., Frid, A., Wirsing, A.J. & Worm, B. (2008) Predicting ecological consequences of marine top predator declines. *Trends in Ecology & Evolution*, **23**, 202–210.

Hudson, L.N., Isaac, N.J.B. & Reuman, D.C. (2013) The relationship between body mass and field metabolic rate among individual birds and mammals. *Journal of Animal Ecology*, **82**, 1009–1020.

Hunsicker, M.E., Ciannelli, L., Bailey, K.M., Buckel, J.A., White, J.W., Link, J.S. *et al.* (2011) Functional responses and scaling in predator–prey interactions of marine fishes: contemporary issues and emerging concepts. *Ecology Letters*, **14**, 1288–1299.

Hutchings, J.A. & Baum, J.K. (2005) Measuring marine fish biodiversity: temporal changes in abundance, life history and demography. *Philosophical Transactions of the Royal Society of London, Series B, Biological Sciences*, **360**, 315–338.

Killen, S.S., Atkinson, D. & Glazier, D.S. (2010) The intraspecific scaling of metabolic rate with body mass in fishes depends on lifestyle and temperature. *Ecology Letters*, **13**, 184–193.

Kleiber, M. (1932) Body size and metabolism. *Hilgardia*, **6**, 315–353.

Kolokotrones, T., Savage, V., Deeds, E.J. & Fontana, W. (2010) Curvature in metabolic scaling. *Nature*, **464**, 753–756.

Meyer, C.G. & Holland, K.N. (2012) Autonomous measurement of ingestion and digestion processes in free-swimming sharks. *Journal of Experimental Biology*, **215**, 3681–3684.

Myers, R.A., Baum, J.K., Shepherd, T.D., Powers, S.P. & Peterson, C.H. (2007) Cascading effects of the loss of apex predatory sharks from a coastal ocean. *Science*, **315**, 1846–1850.

Nagy, K.A. (2005) Field metabolic rate and body size. *Journal of Experimental Biology*, **208**, 1621–1625.

Naito, Y., Costa, D.P., Adachi, T., Robinson, P.W., Fowler, M. & Takahashi, A. (2013) Unravelling the mysteries of a mesopelagic diet: a large apex predator specializes on small prey. *Functional Ecology*, **27**, 710–717.

Parsons, G.R. (1990) Metabolism and swimming efficiency of the bonnethead shark *Sphyrna tiburo*. *Marine Biology*, **104**, 363–367.

Pauly, D., Christensen, V., Dalsgaard, J., Froese, R. & Torres, F. (1998) Fishing down marine food webs. *Science*, **279**, 860–863.

Payne, N.L., Gillanders, B.M., Seymour, R.S., Webber, D.M., Snelling, E.P. & Semmens, J.M. (2011) Accelerometry estimates field metabolic rate in giant Australian cuttlefish *Sepia apama* during breeding. *Journal of Animal Ecology*, **80**, 422–430.

Payne, N.L., van der Meulen, D.E., Gannon, R., Semmens, J.M., Suthers, I.M., Gray, C.A. & Taylor, M.D. (2013) Rain reverses diel activity rhythms in an estuarine teleost. *Proceedings of the Royal Society B, Biological Sciences*, **280**.

Payne, N.L., Taylor, M.D., Watanabe, Y.Y. & Semmens, J.M. (2014) From physiology to physics: are we recognizing the flexibility of biologging tools? *Journal of Experimental Biology*, **217**, 317–322.

Rosa, R. & Seibel, B.A. (2008) Synergistic effects of climate-related variables suggest future physiological impairment in a top oceanic predator. *Proceedings of the National Academy of Sciences of the United States of America*, **105**, 20776–20780.

Rubner, M. (1883) Über den Einfluss der Körpergrösse auf Stoff- und Kraftwechsel. *Zeitschrift für Biologie*, **19**, 536–562.

Ruxton, G.D. (2011) Zoology: why are whales big? *Nature*, **469**, 481.

Savage, V.M., Deeds, E.J. & Fontana, W. (2008) Sizing up allometric scaling theory. *PLoS Computational Biology*, **4**.

Schmidt-Nielsen, K. (1972) Locomotion- energy cost of swimming, flying, and running. *Science*, **177**, 222–228.

Seibel, B.A. (2011) Critical oxygen levels and metabolic suppression in oceanic oxygen minimum zones. *Journal of Experimental Biology*, **214**, 326–336.

Semmens, J.M., Payne, N.L., Huveneers, C., Sims, D.W. & Bruce, B.D. (2013) Feeding requirements of white sharks may be higher than originally thought. *Scientific Reports*, **3**, 1471.

Sepulveda, C.A., Graham, J.B. & Bernal, D. (2007) Aerobic metabolic rates of swimming juvenile mako sharks, *Isurus oxyrinchus*. *Marine Biology*, **152**, 1087–1094.

Stramma, L., Prince, E.D., Schmidtko, S., Luo, J.G., Hoolihan, J.P., Visbeck, M., Wallace, D.W.R., Brandt, P. & Kortzinger, A. (2012) Expansion of oxygen minimum zones may reduce available habitat for tropical pelagic fishes. *Nature Climate Change*, **2**, 33–37.

Ware, D.M. & Thomson, R.E. (2005) Bottom-up ecosystem trophic dynamics determine fish production in the northeast Pacific. *Science*, **308**, 1280–1284.

Watanabe, Y.Y. & Takahashi, A. (2013) Linking animal-borne video to accelerometers reveals prey capture variability. *Proceedings of the National Academy of Sciences of the United States of America*, **110**, 2199–2204.

White, C.R., Blackburn, T.M. & Seymour, R.S. (2009) Phylogenetically informed analysis of the allometry of mammalian basal metabolic rate supports neither geometric nor quarter-power scaling. *Evolution*, **63**, 2658–2667.

White, C.R., Frappell, P.B. & Chown, S.L. (2012) An information-theoretic approach to evaluating the size and temperature dependence of meta-

bolic rate. *Proceedings of the Royal Society B, Biological Sciences*, **279**, 3616–3621.
White, C.R., Phillips, N.F. & Seymour, R.S. (2006) The scaling and temperature dependence of vertebrate metabolism. *Biology Letters*, **2**, 125–127.
Williams, T.M., Estes, J.A., Doak, D.F. & Springer, A.M. (2004) Killer appetites: assessing the role of predators in ecological communities. *Ecology*, **85**, 3373–3384.
Wilson, R.P., White, C.R., Quintana, F., Halsey, L.G., Liebsch, N., Martin, G.R. & Butler, P.J. (2006) Moving towards acceleration for estimates of activity-specific metabolic rate in free-living animals: the case of the cormorant. *Journal of Animal Ecology*, **75**, 1081–1090.
Xiao, X., White, E.P., Hooten, M.B. & Durham, S.L. (2011) On the use of log-transformation vs. nonlinear regression for analyzing biological power laws. *Ecology*, **92**, 1887–1894.

*Received 15 December 2014; accepted 16 February 2015*
*Handling Editor: Carolyn Kurle*

## Supporting Information

Additional Supporting Information may be found in the online version of this article.

**Appendix S1.** Additional notes on mega-flume design and logistics.

**Fig. S1.** Raw traces of dissolved $O_2$ concentrations used to calculate $O_2$ consumption rates during the static respirometry chamber trials.

**Movie S1.** Video of swim trial with 2.1 m 36-kg zebra shark *S. fasciatum* in the mega-flume..